Tunneling Phenomena as a Probe to Investigate Atomic Scale Fluctuations in Metal/Oxide/Metal Magnetic Tunnel Junctions

V. Da Costa, C. Tiusan, T. Dimopoulos, and K. Ounadjela
Institut de Physique et Chimie des Matériaux de Strasbourg, CNRS (UMR 7504) and Université Louis Pasteur, 23 rue du Loess, 67037 Strasbourg Cedex, France
(Received 28 February 2000)

Local transport properties of Al_2O_3 tunnel barriers have been investigated at a nanometric spatial scale with an unconventional near field microscope. Using the tunneling effect, which is extremely sensitive to fluctuations of the barrier parameters (less than 1 to 2 Å), a unique method is introduced to investigate the tunnel barrier quality. This technique provides atomic scale information on the barrier characteristics which cannot be obtained by conventional surface analysis techniques since they are all subject to averaging over surface and depth.

PACS numbers: 85.70.–w, 73.40.Gk, 73.40.Rw

Systems combining metal/oxide interfaces and oxide surfaces constitute a diverse and fascinating class of materials. Their properties play crucial roles in an extremely wide range of physics. The characteristics of high-T_c superconductors, the passivation of metal surfaces against corrosion, the failure of dielectric materials because of an applied voltage, the spin polarized transport in tunnel junctions—all of these phenomena are dependent upon the properties of metal-oxide surfaces and/or the interfaces between metal oxides and other materials. Metal-insulator-metal (MIM) tunnel junctions are nonlinear electronic devices consisting of two metallic electrodes separated by a thin insulating barrier. When the electrodes are composed of ferromagnetic metals, they form magnetic tunnel junctions (MTJ). In a MTJ, the electrical tunnel transport across the insulating barrier is spin dependent and is controlled by the relative orientation of the magnetization in the two magnetic layers adjacent to the tunnel barrier [1]. This property of MIM junctions allow the development of a new generation of sensors for microelectronic devices and magnetic heads for data storage applications, such as magnetic random access memory (MRAM). A successful operation of these junctions requires a chemically homogeneous (free of impurities) insulating barrier as well as little fluctuations of the barrier thickness. Therefore it is important to characterize, spatially resolved, the tunnel barrier and relate it to the macroscopic tunnel magnetoresistance.

While conventional transmission electron microscopy (TEM) and x-ray photoelectron spectroscopy (XPS) studies provide global information on the atomic organization, surface-interface structure, and chemical composition, these techniques give incomplete information on the tunnel barrier quality at the atomic scale because they average over depth and surface. However, the physical relevant parameter in MIM junctions is the tunnel current which is determined by the tunnel barrier quality. More specifically, the tunneling current decreases exponentially with increasing barrier width and/or barrier height. Consequently the preferential conduction channels will be given by those with the highest tunnel current. It is therefore important to investigate the tunneling current spatially resolved.

Here, we demonstrate a unique technique to probe the local tunnel current at the nanoscopic scale using an unconventional direct space near field microscope (barrier impedance scanning microscope, BISM). This technique gives direct information on the correlation between the metal-oxide interfaces at the atomic level. The system studied here is based on Al_2O_3 insulating layers, used as a tunnel barrier in our micronic size tunnel junctions. Two samples, which are found to be identical at the atomic level when examined using standard surface techniques, show large differences both in their transport properties at the nanoscopic spatial scale (tunnel current distribution) and at the microscopic scale (magnetoresistance in micronic sized tunnel junction devices). This result shows the power of the BISM technique to control and optimize the tunnel barrier quality, before making micronic tunnel junction devices by lithography.

The method consists in measuring *in situ* the local tunnel current across the oxide layer with a modified atomic force microscope (AFM) operating with a conducting tip (Fig. 1, top). This technique allows us to map simultaneously the surface roughness and the current intensity transmitted through the oxide layer. In this way we probe directly the physical parameter needed for characterizing the tunnel barrier: the tunnel current. Since quantum tunneling between metal electrodes through an insulating barrier is strongly dependent on the morphology of the metal/insulator interfaces, much effort has been dedicated to optimizing the flatness of these interfaces. The quality of the interfaces in our magnetic tunnel junctions has been ascertained by using a complex buffer layer. It consists in a Cr(1.6 nm)/Fe(6 nm)/Cu(30 nm) trilayer, sputtered on a Si(111) substrate in a high vacuum sputtering system [2]. A magnetically hard subsystem is grown on top of the buffer layer consisting in an artificial ferrimagnet (AFi) Co(1.8 nm)/Ru(0.8 nm)/Co(3 nm) with coercive field of

 0031-9007/00/85(4)/876(4)$15.00

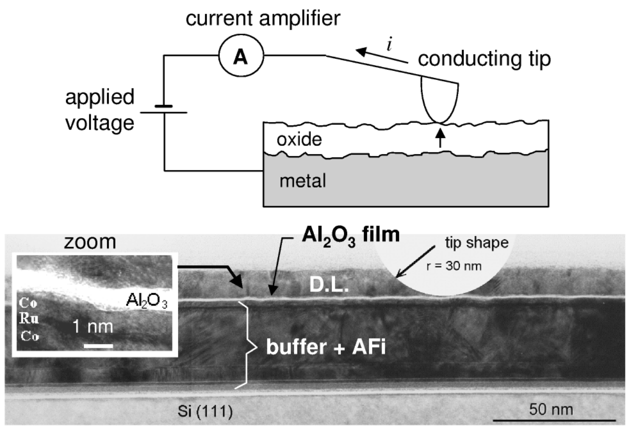

FIG. 1. Cross-section TEM image of a Si(111)/buffer/Co/Ru/Co/Al_2O_3/CoFe/Fe/capping layers. The size of the photo is 257 nm per 80 nm (lateral size comparable to the scan size of the images of Fig. 2). We have intentionally reported a wavy region (zoom at the left) which shows a clear correlation between the two metal/oxide interfaces. Illustration of the tip in contact with the tunnel barrier has been drawn to compare the tip/oxide/metal point contact vs the lateral microscopic size MTJ. On top of the figure is reported a schematic principle of our experimental setup. The conducting AFM tip probes directly the top of the Al oxide surface.

about 400 Oe [2–4]. By using such buffer layers, AFM observations have shown a low surface roughness detected on top of the Al oxide layer (maximum peak to peak and rms values of 7 and 1 Å, respectively). The Al oxide barrier was formed by rf Ar/O_2 plasma oxidation of a previously deposited Al layer on top of the AFi. The oxidation time was optimized with XPS experiments to obtain fully oxidized Al barriers for a given thickness of the as-deposited Al. The optimization of the oxidation time is an important step to avoid over and under oxidation of the barrier, both known to result in detrimental effects on the MTJ's magnetotransport properties [5].

To identify the importance of the correlation between adjacent interfaces, we have prepared two samples differing in the Ar/O_2 pressure during the oxidation procedure, keeping the relative percentage of Ar and O_2 constant: sample I with 5 mTorr and sample II with 50 mTorr Ar/O_2 pressure. For both samples TEM, XPS, and AFM investigations did not indicate any differences in the tunnel barrier quality. A MTJ multilayer stack, typical for both types of samples studied, is illustrated by the cross section TEM image shown in Fig. 1. The Al_2O_3 thin oxide film (white stripe in Fig. 1) has been coated with a magnetically soft bilayer. It consists in a $Co_{50}Fe_{50}$(1 nm)/Fe(6 nm) stack, and acts as a spin detection layer (DL) for electrons injected across the barrier from the hard AFi layer. This TEM image shows that the Al_2O_3 oxide film ($\simeq$11 Å thick) is uniform and continuous in a range of at least several hundreds of nm. No obvious microstructure has been distinguished in the Al_2O_3 layer which would indicate formation of dislocations and/or grain boundaries. Finally, the TEM pictures indicate that the top oxide surface follows the topography of the metal/oxide underlayer, as seen in the zoom of Fig. 1 at least at the resolution of the TEM microscope (TEM has low depth resolution). This means that even when the roughness of each interface is large (compared to the oxide thickness: peak to peak $\simeq$5 Å), the fluctuation in the barrier thickness is reduced to a few Å by the correlation of the roughness of the lower and top interfaces which may lead to small variation of the tunnel current. The TEM and XPS are techniques commonly used to characterize the structural and chemical quality of the tunnel barrier as a whole. Conventional AFM provides information only on the spatial distribution of the top surface roughness. However, as shown in the following, these techniques are unable to provide information on the spatial homogeneity of the tunnel barrier width and height.

This latter point has been addressed by performing local transport measurements at a nanoscopic scale. The local measurements were performed just after the growth of the Al oxide layer. The structure of the investigated sample is then as follows: Si(111)/buffer/AFi/Al_2O_3, the detection layer was not deposited, thus the oxide is on the top surface. The conducting AFM tip (Si_3N_4 coated with 30 nm thick TiN) *probes* directly the top of the Al oxide surface and is used as the second electrode of the tunnel junction. The topography was obtained by standard AFM measurements in *contact mode* and at constant force. A bias voltage (typically 1 V) was applied between the bottom metallic layer and the conducting tip, so as to generate a current flow from the sample to the probe (see sketch shown in Fig. 1). Other details on the technique can be found elsewhere [6–8].

Figures 2(c) and 2(d) show 200×200 nm^2 current maps recorded on samples I and II. The measured topography images [Fig. 2(a) and 2(b)] are similar for both films and reveal extremely smooth surfaces (rms $\simeq$ 1 Å). The image Fig. 2(c) represents the cartography of the tunnel current of a higher quality tunnel barrier corresponding to sample I: the Ar/O_2 pressure (5 m Torr) and the oxidation time are well optimized. Note the variation of the tunnel current which varies locally by no more than 2 orders of magnitude. The blue background identifies regions with tunnel current in the order of 100 pA, while the green spots are indicative of higher tunnel current zone (1–10 nA). The small amplitude of the measured current is due to the small contact area between the tip and the insulating barrier. The contact spot area is estimated to be about 100 Å^2. In order to illustrate this resolution the relative tip size (radius of 30 nm) with respect to the scanned area is drawn on top of the TEM image of the complete MTJ (Fig. 1).

Figure 2(d) shows the typical tunnel current map for sample II with a less optimized tunnel barrier. As

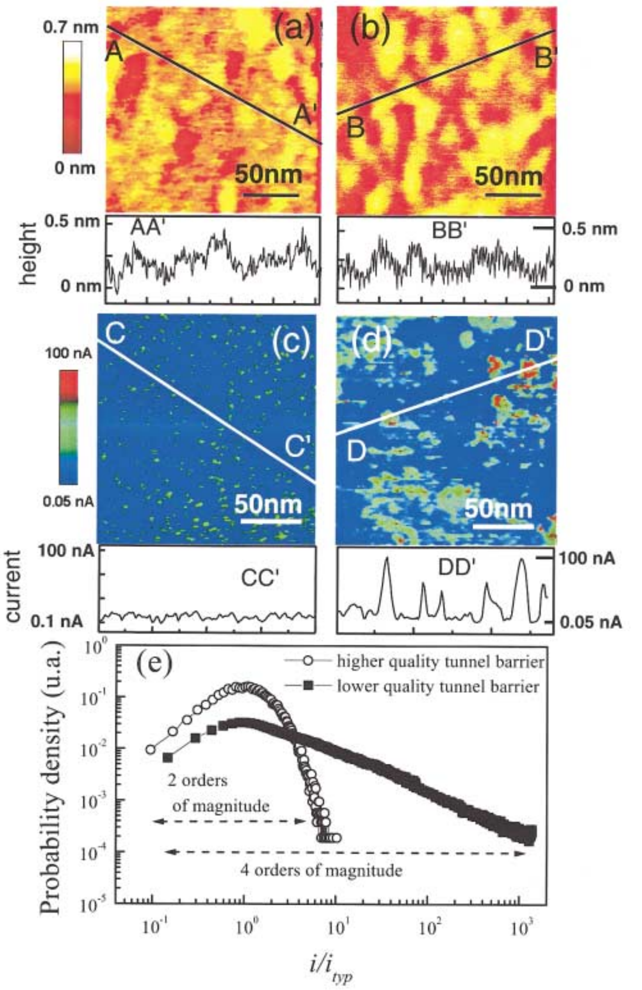

FIG. 2 (color). The 200 × 200 nm^2 size (a),(b) topographical and (c),(d) current images performed on an Al_2O_3. (a),(c) and (b),(d) images are simultaneously acquired. (a),(c) and (b),(d) are, respectively, measured on higher quality (sample I) and lower quality (sample II) insulating barriers. Also displayed are height and current profiles along lines shown in the image. (e) represents the current intensity distributions for the higher (− ∘ − sample I) and for the lower (−■− sample II) quality insulating barriers.

already mentioned, the oxidation procedure does not seem to affect the topography of the films when comparing the peak to peak and rms values of the oxide surface of both samples [see Figs. 2(a) and 2(b)]. However, the tunnel current cartography shows a drastic difference when compared to sample I with current inhomogeneity over 4 orders of magnitude. Note on the image, the red spots indicate current intensities up to 100 nA. Even in these hot spots, the current has still a tunneling character and not a shortcut current. This aspect is verified by measuring nonlinear I-V characteristics. From the current cartography, we have calculated the statistical distributions of local currents to quantify the quality of the insulating barrier. Previous works [9,10] have shown that a broad distribution of the current intensity with a long tail characterizes significant spatial variations of the oxide properties (thickness fluctuation of about 1 to 2 Å). On the other hand, a narrow current distribution indicates very small spatial variations (less than 0.1 Å) of the tunnel barrier parameters and is a signature of very high homogeneity in the physical parameters of the tunnel barrier. Figure 2(e) shows the distributions of local currents for both samples. For sample I the current distribution decreases quickly for the larger currents. It appears that the reduced current i/i_{typ} intensities (i_{typ} is the value for which the current distribution is maximum) vary from 0.1 to 10, so the tunnel current variations extend to *only* 2 orders of magnitude. This indicates that the buried metal-oxide interface is correlated with the top surface at the angstrom scale. For sample II the values of tunnel current variations extend over 4 decades ($i/i_{\mathrm{typ}} = 0.1$ to 1000). The current distribution curve is broad with a relatively slow decrease for larger current intensities.

Both fluctuations of the barrier height and width would coexist and have similar consequences on the statistical properties of quantum tunneling. For instance, considering only the fluctuation of the barrier width enables one to extract quantitative values for thickness fluctuation. As discussed in Refs. [9,10], a log-normal model of current distribution could be applied to estimate the oxide thickness fluctuation σ. Thus, we obtain for samples I and II, $\sigma = 0.3$ Å and $\sigma = 1.6$ Å, respectively; see note in [11] for details. This result suggests that the high partial pressure applied during the oxidation of the Al affects the correlation between the top and bottom interfaces of the oxide layer without deteriorating the smoothness of the top oxide surface. Note that the loss in correlation is small enough to be undetectable using cross section TEM experiments.

Whether such small fluctuation in barrier physical parameters can be detected using complementary investigations has been addressed by (i) measuring the tunnel magnetoresistance of micronic junctions as well as (ii) purposely creating breakdowns on the surface of the films.

To allow a comparison between both oxidation conditions for samples I and II, tunnel magnetoresistances (TMR) have been measured on microscopic tunnel junctions. The TMR is the only pertinent parameter to characterize the quality of the spin polarized tunnel current in a MTJ. The amplitude of the TMR signal reflects the atomic organization of the interfaces due to the local electronic structure, the tunneling mechanism, and the fluctuations in barrier parameters. For this purpose, complete stacks have been patterned by UV lithography into large arrays of square shaped junctions (10 × 10 μm^2). Several junctions with high quality tunnel barrier prepared in the same conditions as sample I, measured at room temperature using a conventional four-point technique with a dc voltage source, present large tunnel magnetoresistance which varies from 26% to 30%. However, junctions with less well optimized tunnel barrier (equivalent to sample II) present much lower TMR values varying from 11% to a maximum of 16%. These results show that averaging at the

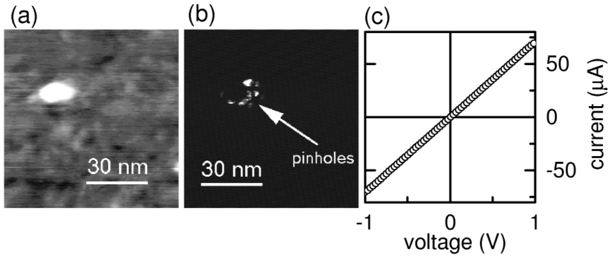

FIG. 3. Images of pinholes intentionally created by applying a large voltage. (a) Topography of the surface, (b) current image, and (c) the current-voltage characteristic measured with the tip localized on the pinhole.

microscopic scale the tunnel transport properties reflects implicitly the Al_2O_3 tunnel barrier quality measured with nanometer resolution.

Another type of investigation is to compare the stability of both types of surfaces to dielectric breakdowns. We have intentionally created the breakdowns on top of the oxide surface by applying high voltage between the tip and the sample using the same setup with the tip at rest. Interestingly, the pinhole defects at the origin of the breakdown are created for both oxide surfaces at similar bias voltage (in the range of 6 V, electric field $E = 5.5 \times 10^9$ V/m for a tunnel barrier of 11 Å) and it seems not to depend critically on the quality of the oxide layer. These defects are clearly evidenced in Fig. 3 which show localized current spots with very high current intensities, usually in the range of 50 μA for 1 V, 3 orders of magnitude higher than the highest detected tunnel current. Moreover, when the tip probes the pinhole, the current response is characterized by a linear I-V behavior indicating an electrical metal transport conduction; see Fig. 3(c). This experiment reveals two interesting features: (i) the breakdowns appear at a bias voltage around 6 V, 6 times higher than the electrical breakdowns observed in micronic junctions [12]. This difference can be explained because the micronic junction probes a large number of high current nanometric sites enhancing the probability to have those sites producing a lower voltage breakdown. Since the size of contact (tip-sample) in our experiment is in the range of 100 Å^2, this confirms that decreasing the size of the tunnel junction will enhance their stability to dielectric breakdowns vs bias voltage. (ii) More importantly, the breakdown appears in the same range of bias voltage for both oxide surfaces which indicates that despite the large contrast observed in the spatial distributions of tunnel currents between samples I and II, only very tiny spatial fluctuations of tunnel barrier thickness, more likely in the angstrom range, can account for these differences. This can be explained by the inversely proportional relationship between electric field for breakdown vs barrier width compared to the exponential dependence of the tunnel current with the barrier width, making the electrical field breakdowns less sensitive to spatial fluctuations of barrier physical parameters.

In summary, the quality of Al oxide layers, used as tunnel barriers in MTJ devices, has been investigated in terms of tunnel current homogeneity, by using a modified AFM/STM technique (STM: scanning tunneling microscopy). This technique provides a unique way to make an *electrical mapping* of the tunnel barriers before building micronic sized magnetic tunnel junctions. Thus, we are able to test locally the quality of the barrier, to examine the presence of possible *electrical defects* which would alter the magnetoresistive response of the MTJ device. More importantly, we have succeeded to detect fluctuations in the oxide barrier quality, from sample to sample, which were not accessible using any other surface techniques. These fluctuations are reflected in the TMR signal of the MTJ. Finally, the dielectric breakdown voltage does not seem to be strongly dependent on the quality of the oxide layer in contrast to the local tunnel current mapping.

The authors gratefully thank G. Würtz, G. Ehret, M. Hehn, F. Bardou, and U. Ebels. This work was supported by the EC Framework IV Materials Technology Programme (Contract No. BRPR-CT98-0657), the *Dynaspin* program, *TMR* network (Contract No. FMRX-CT97-0147), and *Nanomem* Programme (No. IST-1999-13741).

[1] J.S. Moodera, L.R. Kinder, T.M. Wong, and R. Meservey, Phys. Rev. Lett. **74**, 3273 (1995); T. Miyazaki and N. Tezuka, J. Magn. Magn. Mater. **139**, L231 (1995).
[2] C. Tiusan, M. Hehn, K. Ounadjela, Y. Henry, J. Hommet, C. Meny, H.A.M. van den Berg, L. Baer, and R. Kinder, J. Appl. Phys. **85**, 5276 (1999).
[3] H.A.M. van den Berg, W. Clemens, G. Gieres, G. Rupp, M. Vieth, J. Wecker, and S. Zoll, J. Magn. Magn. Mater. **165**, 524 (1997).
[4] C. Tiusan, T. Dimopoulos, K. Ounadjela, M. Hehn, H.A.M. van den Berg, V. da Costa, and Y. Henry, Phys. Rev. B **61**, 580 (2000).
[5] J.S. Moodera, E.F. Gallagher, K. Robinson, and J. Nowak, Appl. Phys. Lett. **70**, 3050 (1997).
[6] F. Houzé, R. Meyer, O. Schneegans, and L. Boyer, Appl. Phys. Lett. **69**, 1975 (1996).
[7] M.A. Lantz, S.J. O'Shea, and M.E. Welland, Rev. Sci. Instrum. **69**, 1757 (1998).
[8] V. Da Costa, F. Bardou, C. Beal, Y. Henry, J.P. Bucher, and K. Ounadjela, J. Appl. Phys. **83**, 6703 (1998).
[9] F. Bardou, Europhys. Lett. **39**, 239 (1997).
[10] V. Da Costa, Y. Henry, F. Bardou, M. Romeo, and K. Ounadjela, Eur. Phys. J. B **13**, 297 (2000).
[11] Experimental data were fitted with a log-nomal distribution which gives the parameters α' and β where α' is a scale factor and $\beta = \sigma/\lambda$ is a fluctuation parameter [9,10]. σ and λ indicate, respectively, the fluctuation of the barrier thickness and the attenuation length in the barrier. To calculate σ, we set $\lambda = 0.6$ Å which is a good value for Al_2O_3 tunnel barriers.
[12] W. Oepts, H.J. Verhagen, and W.J.M. de Jonge, Appl. Phys. Lett. **73**, 2363 (1998).